CONTROL OF THE EXHAUST GAS EMISSIONS DURING THE WARM-UP PROCESS OF A TWC-EQUIPPED SI ENGINE

Giovanni Fiengo *Luigi Glielmo** Stefania Santini* **Gabriele Serra***

*Computer and System Engineering Department
Università di Napoli Federico II, Naples, Italy.
E-mail: {gifiengo, stsantin}@unina.it
** School of Engineering Università del Sannio, Benevento, Italy.
E-mail: glielmo@unisannio.it.
*** Magneti Marelli Powertrain Division, Bologna, Italy*

Abstract: This paper introduces a model-based controller designed to minimize the total unburned hydrocarbons produced by the internal combustion engine and processed by the three way catalytic converter, during the warm-up period.
We assume to feed back the temperature of the exhaust gas; having in mind to decouple the control of combustion from the control of intake manifold, we assumed as controllable inputs the flow of air and fuel *into the cylinder* and the spark advance. The outputs are the total unburned hydrocarbons pre and post converter.

1. INTRODUCTION

Nowadays, every new motor vehicle is equipped with a three-way catalytic converter (TWC) and an emissions control system aimed at reducing the pollutants emitted from spark ignition internal combustion engines (SI-ICE). The action of the TWC concurs to pull down the concentrations of carbon monoxide, nitrogen oxides and unburned hydrocarbons in exhaust gases. The chemical reactions inside the TWC proceed simultaneously, provide the catalytic converter is "sufficiently" heated and the composition of the mixture feeding the engine is maintained at stoichiometry by the control strategy governing air and fuel supplied to the engine.

Currently, new and stricter anti-pollution norms in automotive field request an on-line optimization of engine control strategies during every driving condition. In particular, a still open problem is the pollutant reduction during the thermal transient, when the converter does not yet work correctly and, therefore, a large quantitative of injurious substances is emitted.

From what above, the design of these new real time applications, as warm-up controllers and on board diagnostic systems (see, for example, Fiengo et al. (2001)), starts from reliable mathematical models of the dynamic behavior of the SI-ICE and the catalyst.

In this work, based on simplified phenomenological models of the engine combustion and the catalytic converter presented in Fiengo et al. (2002), a control strategy will be proposed, aimed at minimizing the total unburned hydrocarbons produced by the engine and not processed by the catalyst during the warm-up period. This controller is computed by solving on-line an approximate linear quadratic optimization problem.

2. CONTROL ORIENTED MODELS

2.1 Internal Combustion Engine

The scheme in figure 1 represents the model of the internal combustion engine. It was presented

in Fiengo et al. (2002) and in the following it will be briefly illustrated.

The model describes the combustion process assuming that air and fuel entering the combustion chamber can be directly assigned. Two inputs represent the physical quantities entering the cylinder, through air mass flow rate ($\dot{m}_a$ [g/sec]) and air/fuel ratio (λ [/]); other inputs are the spark advance (θ [deg]), the engine speed (n [rpm]) and the temperature of the coolant (T_{cool} [C]). The output is the total unburned hydrocarbons (THC_{pre} [g/sec]); the state of the model is the exhaust gas temperature (T_{FG} [C]). In the following the model blocks are briefly described.
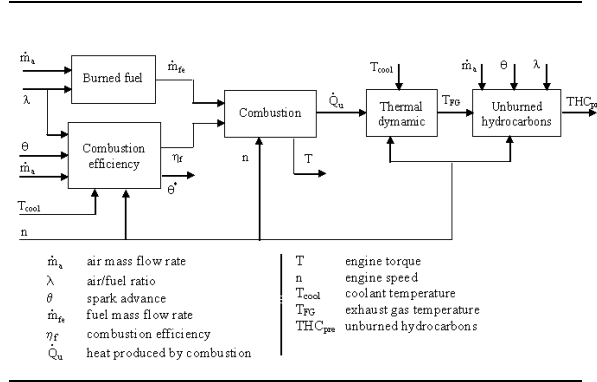

Fig. 1. Internal combustion engine

Burned fuel It computes the fuel charge ($\dot{m}_{\text{fe}}$ [g/sec]) actually burnt during the combustion:

$$\dot{m}_{\text{fe}} = \frac{\dot{m}_a}{\lambda_{\text{ST}}} \times \begin{cases} \dfrac{1}{\lambda} & \text{when} \quad \lambda \geq 1 \\[2mm] 1 & \text{when} \quad \lambda < 1 \end{cases} \qquad (1)$$

where λ_{ST} is the stoichiometric value of the air-fuel ratio.

Combustion efficiency It estimates the efficiency of the engine (η_f [%]) in transforming the chemical energy of the fuel into mechanical energy through the combustion:

$$\eta_\lambda = c_0 + \theta \left(c_1 \lambda^2 - c_2 \lambda\right), \qquad (2a)$$
$$\eta_{\text{AV}} = 1 - c_3(\theta - \theta^*)^2, \qquad (2b)$$
$$\eta_f = \eta_\lambda \cdot \eta_{\text{AV}}, \qquad (2c)$$

where θ^* is the nominal value of the spark advance for the production of the torque from the combustion and it is a nonlinear function of the engine operative point $\theta^* = f(n, \dot{m}_a, T_{\text{cool}})$.

Combustion It estimates the mean indicated torque generated by the combustion (T [Nm]) and the heat produced by the combustion ($\dot{Q}_u$ [W]) warming the exhaust gas:

$$T = \frac{\eta_f \dot{m}_{\text{fe}} Q_{\text{HV}}}{n}, \qquad (3a)$$
$$\dot{Q}_u = \beta(t)\left(1 - \eta_f\right) \dot{m}_{\text{fe}} Q_{\text{HV}}, \qquad (3b)$$

where Q_{HV} is the low heat value of the fuel [J/g] and β describes the time-varying partition of thermal energy directed toward both the engine mechanical components and exhaust gas.

Thermal dynamic It models the dynamical behavior of the exhaust gas temperature:

$$\dot{T}_{\text{FG}} = a_0 \dot{Q}_u - a_1 n(T_{\text{FG}} - T_{\text{cool}}). \qquad (4)$$

Unburned hydrocarbons It calculates the total unburned hydrocarbons (THC_{pre}) at the exhaust pipe as a function of the feedgas temperature (T_{FG}), air mass flow rate ($\dot{m}_a$), spark advance (θ), engine speed (n) and air/fuel ratio (λ).

2.2 Three Way Catalytic Converter

In figure 2 is shown the block diagram of a simple phenomenological TWC dynamic model presented in Fiengo et al. (2002). It was developed for control purposes and captures the phenomenon of the oxygen storage. The oxygen-storage is a key mechanism that enhances the catalyst activity helping the catalyzed oxidation-reduction reactions: during transients, in presence of oxygen excess, there is an oxygen chemiadsorption on the catalyst, while in conditions of defect, there is a release.
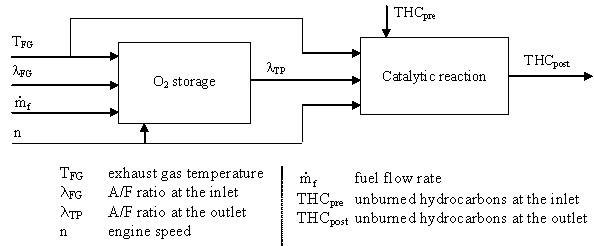

Fig. 2. Three way catalytic converter

It is important to note that we use the feedgas temperature (T_{FG}) as an indirect indicator of the catalyst temperature. This hypothesis allows to not model the temperature dynamics inside the TWC so reducing the system order. In the following the model blocks will be briefly introduced.

Oxygen Storage The oxygen storage phenomenon is modelled by two actions aimed at correcting the quantity of oxygen in the gas at the inlet of the catalyst, trying to reach the optimal value for the catalytic reactions, the stoichiometric point.

We compute the fraction per unit of time of oxygen capacity that is effectively stored in lean condition or released in rich condition $\dot{\Theta}_{\mathrm{cor}}$ as follows:

$$\dot{\Theta}_{\mathrm{cor}} = (\dot{\Theta}_{\mathrm{FG}} - \dot{\Theta}_{\mathrm{St}}) \cdot g(T_{\mathrm{FG}}) \cdot \begin{cases} f_L(\Theta) & \lambda_{\mathrm{FG}} \geq 1 \\ f_R(\Theta) & \lambda_{\mathrm{FG}} < 1 \end{cases} \tag{5}$$

where $\dot{\Theta}_{\mathrm{FG}}$ and $\dot{\Theta}_{\mathrm{St}}$ are the fraction per unit of time of the total oxygen quantity respectively present in the feedgas and, ideally, at the stoichiometric value; Θ is the fraction of oxygen capacity occupied in the TWC; $g(T_{\mathrm{FG}})$ is a function that models how the feedgas temperature affects the TWC efficiency; and the functions $f_L(\Theta)$ and $f_R(\Theta)$ determine how much of the surplus or deficit oxygen can be respectively stored or released depending on the catalyst state.

After computing $\dot{\Theta}_{\mathrm{cor}}$, it is possible to compute the fraction of oxygen capacity per unit of time in the gas after this first correction, $\dot{\Theta}_{\mathrm{FG}_{\mathrm{cor}}}$, and the corresponding A/F ratio, $\lambda_{\mathrm{FG}_{\mathrm{cor}}}$:

$$\dot{\Theta}_{\mathrm{FG}_{\mathrm{cor}}} = \dot{\Theta}_{\mathrm{FG}} - \dot{\Theta}_{\mathrm{cor}}, \tag{6a}$$

$$\lambda_{\mathrm{FG}_{\mathrm{cor}}} = \frac{\dot{\Theta}_{\mathrm{FG}_{\mathrm{cor}}} C}{0.23 \, \dot{m}_{\mathrm{f}} S}, \tag{6b}$$

where C is the catalyst capacity.

A second correction is modelled by a first order linear system

$$\dot{\lambda}_{\mathrm{aux}} = -\frac{\lambda_{\mathrm{aux}}}{\tau(\lambda_{\mathrm{FG}}, \lambda_{\mathrm{aux}}, T_{\mathrm{FG}})} + \frac{\lambda_{\mathrm{FG}_{\mathrm{cor}}}}{\tau(\lambda_{\mathrm{FG}}, \lambda_{\mathrm{aux}}, T_{\mathrm{FG}})}, \tag{7}$$

where $\tau(\lambda_{\mathrm{FG}}, \lambda_{\mathrm{aux}}, T_{\mathrm{FG}})$ is the time constant, depending on the air/fuel ratio of the gas at the inlet and the outlet of the catalyst, and the feedgas temperature.

Now it is possible to determine the change of oxygen capacity occupied in the TWC, in according to:

$$\dot{\Theta} = \begin{cases} \dot{\Theta}_{\mathrm{FG}} - \dot{\Theta}_{\mathrm{aux}} & \Theta \in (0,1) \\ \max\{0, \dot{\Theta}_{\mathrm{FG}} - \dot{\Theta}_{\mathrm{aux}}\} & \Theta = 0 \\ \min\{0, \dot{\Theta}_{\mathrm{FG}} - \dot{\Theta}_{\mathrm{aux}}\} & \Theta = 1 \end{cases} \tag{8}$$

where $\dot{\Theta}_{\mathrm{aux}}$ is the corresponding fraction of oxygen capacity per unit of time present in the gas at the outlet of the catalyst.

Finally the air-fuel ratio at the tailpipe, λ_{TP} (model output), is described as follows:

$$\lambda_{\mathrm{TP}}(t) = \lambda_{\mathrm{aux}}(t - \Delta(t)), \tag{9}$$

where Δ is the transport delay of the gas, depending on an average value of the air mass flow rate.

Catalytic Reactions The simplified kinetic model has one output (the mass flow rate of the un-

burned hydrocarbons at the outlet of the TWC, THC_{post} [g/sec]), five inputs (the mass flow rate of the unburned hydrocarbons at the inlet of the TWC, $\mathrm{THC}_{\mathrm{pre}}$ [g/sec]; the engine speed, n [rpm]; the fuel flow rate, $\dot{m}_f$ [g/sec]; the air/fuel ratio of the gas corrected by the oxygen storage phenomenon, λ_{TP} [/]; the feedgas temperature, T_{FG} [C]) and two states (the mass flow rate of the unburned hydrocarbons in the middle of the catalyst, $\mathrm{THC}_{\mathrm{md}}$ [g/sec] and at the end, $\mathrm{THC}_{\mathrm{post}}$ [g/sec]):

$$\dot{\mathrm{THC}}_{\mathrm{md}} = -K_1 n(\mathrm{THC}_{\mathrm{md}} - \mathrm{THC}_{\mathrm{pre}}) \\ - R_{\mathrm{md}}(T_{\mathrm{FG}}, \mathrm{THC}_{\mathrm{md}}, \dot{m}_f, \lambda_{\mathrm{TP}}),$$

$$\dot{\mathrm{THC}}_{\mathrm{post}} = -K_2 n(\mathrm{THC}_{\mathrm{post}} - \mathrm{THC}_{\mathrm{md}}) \\ - R_{\mathrm{post}}(T_{\mathrm{FG}}, \mathrm{THC}_{\mathrm{post}}, \dot{m}_f, \lambda_{\mathrm{TP}});$$

where $R_i = R_i(T_{\mathrm{FG}}, \mathrm{THC}_i, \dot{m}_f, \lambda_{\mathrm{TP}})$ are the reaction rates, $i = \mathrm{md}, \mathrm{post}$.

3. WARM-UP CONTROL

The goal of the control strategy is to command the engine minimizing the polluting emissions at the outlet of the three way catalytic converter.

Here the main idea is to use the spark advance (θ) to increase the feedgas temperature. On the other side this causes a performance loss for the torque that is compensated increasing the air mass flow rate ($\dot{m}_a$). Supposing to measure the exhaust gas temperature, we realize a feedback loop around the engine system (see figure 3) that allows to shorten the warm-up duration. The action is bounded to produce same extra-pollution in the first seconds of engine working. This is caused by the non optimal combustion due to the peculiar use of spark angle and air mass flow rate. Extra-pollution will be compensated by earlier activation of catalytic reactions.

From above it is apparent that TWC system is not included in optimal control loop since no sensor exists (or is commercially available) at this moment to measure the unburned hydrocarbons on line. Its model is used to off-line tune the parameters, as explained later.

In conclusion the control strategy must find an optimal balance between earlier TWC activation and extra-pollution production.

The engine control problem was treated as an optimal control problem (see equation (18) in the Appendix, section 5), where we suppose the spark angle (θ) to be the controllable input, and air mass flow rate ($\dot{m}_a$), air/fuel ratio (λ), engine speed (n) and coolant temperature (T_{cool}) to be uncontrollable inputs; we indicate the states and the inputs of the engine system as follows
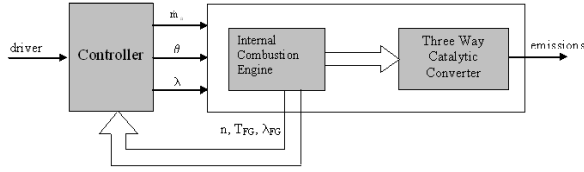
Fig. 3. Control scheme

$$x = T_{\text{FG}}; \qquad u = \theta; \qquad \nu = \begin{pmatrix} \dot{m}_a \\ \lambda \\ n \\ T_{\text{cool}} \end{pmatrix}. \quad (11)$$

This choice is due to the following considerations:

- The air mass flow rate $(\dot{m}_a)$ is used to produce the requested engine torque and thus maintain the performances unchanged. It is computed as follows

$$\dot{m}_a = \frac{\lambda_{\text{ST}} P_{\text{rif}}}{\eta_f Q_{\text{HV}}} \times \begin{cases} \lambda \text{ when } \lambda \geq 1 \\ \\ 1 \text{ when } \lambda < 1 \end{cases} \quad (12)$$

  where $P_{\text{rif}} = T_{\text{rif}} n$ is the reference power, depending on the torque T_{rif} demanded by the driver.
- Since this control strategy must work during the cold start and the warm-up period, when the oxygen sensors are badly working and so a good A/F control is not possible to realize, the air/fuel ratio in the cylinder (λ) is not used as a controllable input.
- The engine speed (n) is determined by the torque commanded by the driver.
- The coolant temperature (T_{cool}) is physically an uncontrollable input.
- Intake manifold dynamics will be taken into account in a successive step when designing a controller for throttle and fuel injectors.

In this work a secondary air pump on the exhaust manifold is not considered. This device, inserted in the exhaust pipe, allows to burn the hydrocarbons contained in feedgas, thus increasing the TWC temperature. We are going to exploit the effectiveness of this technique in future activity in this research field.

Letting $(\overline{T}_{\text{FG}}, \overline{\theta}, \overline{\dot{m}}_a, \overline{\lambda} = 1, \overline{n}, \overline{T}_{\text{cool}})$ be a generic point in the state and input space and $\overline{t}$ a generic time instant, we can calculate the linearized system (from model equations (1) – (4)) as follows

$$\delta \dot{T}_{\text{FG}} = -a_1 \overline{n} \, \delta T_{\text{FG}} + a_0 \frac{\partial \overline{Q}_u}{\partial \theta} \delta \theta$$
$$+ a_0 \frac{\partial \overline{Q}_u}{\partial \dot{m}_a} \delta \dot{m}_a + a_0 \frac{\partial \overline{Q}_u}{\partial \lambda} \delta \lambda +$$
$$+ \left[a_0 \frac{\partial \overline{Q}_u}{\partial n} - a_1 (\overline{T}_{\text{FG}} - \overline{T}_{\text{cool}}) \right] \delta n + \quad (13)$$
$$+ \left[a_0 \frac{\partial \overline{Q}_u}{\partial T_{\text{cool}}} + a_1 \overline{n} \right] \delta T_{\text{cool}},$$

where the the overlined terms indicate functions calculated in the linearization point. So, the linearized system (13) can be rewritten as

$$\delta \dot{x} = A \delta x + Bu + [f(\overline{x}, \overline{u}, \overline{\nu}) + \Gamma \delta \nu - B \overline{u}] ; \quad (14)$$

where the dynamic matrices are

$$A = -a_1 \overline{n}, \quad (15a)$$

$$B = a_0 \frac{\partial \overline{Q}_u}{\partial \theta}, \quad (15b)$$

$$\Gamma = \begin{pmatrix} a_0 \dfrac{\partial \overline{Q}_u}{\partial \dot{m}_a} \\ a_0 \dfrac{\partial \overline{Q}_u}{\partial \lambda} \\ \left[a_0 \dfrac{\partial \overline{Q}_u}{\partial n} - a_1 (\overline{T}_{\text{FG}} - \overline{T}_{\text{cool}}) \right] \\ \left[a_0 \dfrac{\partial \overline{Q}_u}{\partial T_{\text{cool}}} + a_1 \overline{n} \right] \end{pmatrix}^T ; \quad (15c)$$

and the nonlinear function, computed in the linearization point, is

$$f(\overline{x}, \overline{u}, \overline{\nu}) = a_0 \overline{Q}_u - a_1 \overline{n}(\overline{T}_{\text{FG}} - \overline{T}_{\text{cool}}). \quad (16)$$

Finally, we need the state and input signals to track. For the spark angle we use its nominal value θ^*, while for the feedgas temperature, which is unconstrained, its reference $(\tilde{T}_{\text{FG}})$ is a parameter of the controller to be set.

Now, based on linearization, the suboptimal control law can be obtained solving the corresponding differential Riccati equation (see Appendix 5 for mathematical details). Moreover, in order to reduce the computational complexity of the control algorithm, here we employ algebraic equations as follows

$$PA + A^T P - PBR^{-1}B^T P + Q = 0 \quad (17a)$$
$$(A - BR^{-1}B^T P)^T b - Q(\tilde{x} - \overline{x}) +$$
$$+ P\left[f(\overline{x}, \overline{u}, \overline{\nu}) + \Gamma \delta \nu + B(\tilde{u} - \overline{u}) \right] = 0 \quad (17b)$$

The linearized system, and consequently the matrices P and b obtained by equations (17), is computed whenever the norm of the deviation vector $(\delta x, \delta u, \delta \nu)$ is bigger than a threshold, typically a percentage of the norm of the vector $(\overline{x}, \overline{u}, \overline{\nu})$.

Determined the matrices P and b, the control input u_{subopt} is computed as (22). The parameters

of the controller (the weight matrices Q and R and the reference signal $\tilde{T}_{FG}$) are obtained solving an optimization problem through a purposely designed genetic algorithm (see Davis (1991)): minimize the unburned hydrocarbons produced at the outlet of the catalytic converter. The procedure is based on the TWC model introduced in section 2.2.

The performances of the "warm-up controller", described in this paper, are compared with experimental data referring to an engine and a TWC controlled by a strategy currently implemented in a commercial ECU during an ECE drive cycle. In the following we refer to this commercial controller as "standard controller". The system inputs, not computed by warm-up controller (air fuel ratio, engine speed and coolant temperature) are obtained from data.

The following figures report the system outputs when the standard controller (dashed line) and the warm-up controller (22) (solid line) is applied. In these figures, the vertical line points out the time instant when the temperature goal of the warm-up controller is reached and, hence, the standard controller is switched on. The deviation in trends that exist in figure 4 after the vertical line is only numerical caused by different integration steps.

Figures 6 and 7 show the time history of pre and post-catalyst unburned hydrocarbons integral value respectively when the warm-up controller is applied (solid line) and not applied (dotted line). The results show that the unburned hydrocarbons produced by the engine combustion remain almost unchanged: the integral of the THC with the standard control is 3.36g and with the warm-up control is 3.38g. On the other hand, the unburned hydrocarbons at the outlet of the catalyst decrease by 21.5% (0.77g with the standard control, 0.60g with the warm-up control).
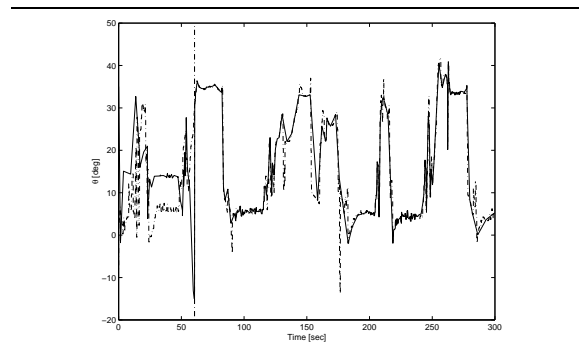

Fig. 4. Spark advance, θ, when the warm-up controller is applied (solid line) and not applied (dotted line)
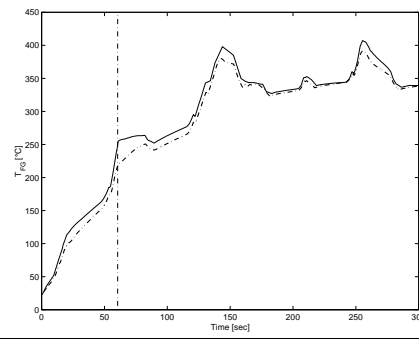

Fig. 5. Exhaust gas temperature, T_{FG}, when the warm-up controller is applied (solid line) and not applied (dotted line)
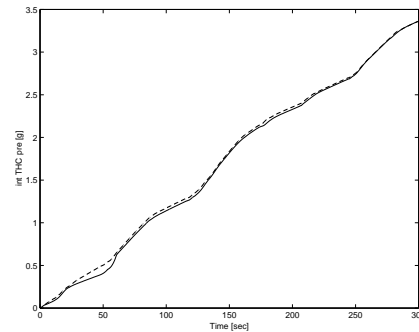

Fig. 6. Time history of the integral value of pre-catalyst unburned hydrocarbons respectively when the warm-up controller is applied (solid line) and not applied (dotted line).
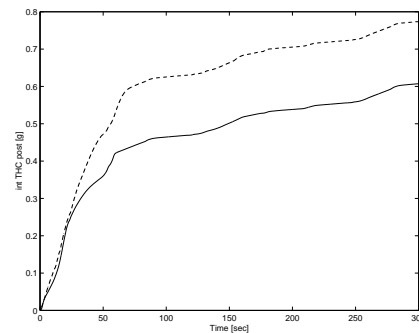

Fig. 7. Time history of the integral value of post-catalyst unburned hydrocarbons respectively when the warm-up controller is applied (solid line) and not applied (dotted line).

4. CONCLUSION

In this paper a first version of a warm-up control strategy for the cascade SI-ICE/TWC was presented. The procedure was designed and tested by simulation on experimental data furnished by Magneti Marelli. Future work in this research field will concern with refinements of the control strategy and implementation of the controller on a vehicle. Moreover, in the future the possibility to use other control variable, instead of the only spark advance angle, will be exploited.

5. APPENDIX

5.1 *A Nonlinear Finite Horizon Sub-Optimal Control*

Let consider the following optimal control problem for nonlinear systems

$$\dot{x} = f(x, u, \nu), \qquad x(0) = x_0, \qquad (18a)$$

$$\min_{u(.)} V = \min_{u(.)} \frac{1}{2} \int_0^T \left[(x - \tilde{x})^T Q (x - \tilde{x}) + \right.$$

$$\left. + (u - \tilde{u})^T R (u - \tilde{u}) \right], \qquad (18b)$$

where x is the variable state, u is the controllable input and ν is an uncontrollable input. Since, on many occasions, finding the exact solution to this nonlinear optimal control problem is practically unfeasible, we illustrate a suboptimal procedure based on successive linearization of the problem. Our approach resembles receding horizon techniques, such as in Mayne and Michalska (1990) and in Chen and Allgöwer (1998).

Let $\overline{x}$, $\overline{u}$ and $\overline{\nu}$ be a generic point in the state space and in the input space, and compute the linearized system at this point

$$\delta \dot{x} = A \delta x + B \delta u + \Gamma \delta \nu + f(\overline{x}, \overline{u}, \overline{\nu}) \qquad (19)$$

where

- δx, δu and $\delta \nu$ are the deviations from the chosen fixed point $(\overline{x}, \overline{u}, \overline{\nu})$;
- A, B and Γ are the jacobian matrices.

The objective functional (18b) becomes

$$V = \frac{1}{2} \int_0^T \left[(\delta x - (\tilde{x} - \overline{x}))^T Q (\delta x - (\tilde{x} - \overline{x})) + \right.$$

$$\left. + (u - \tilde{u})^T R (u - \tilde{u}) \right] dt, \qquad (20)$$

where $(\tilde{x} - \overline{x})$ is the new signal to be tracked. Finally, substituting $u = \overline{u} + \delta u$ into (19), we obtain:

$$\delta \dot{x} = A \delta x + B u + [f(\overline{x}, \overline{u}, \overline{\nu}) + \Gamma \delta \nu - B \overline{u}]. \quad (21)$$

The optimal control for the linearized system is:

$$-\dot{P} = PA + A^T P - PBR^{-1}B^T P + Q, \quad P(T) = 0,$$

$$-\dot{b} = (A - BR^{-1}B^T P)^T b +$$

$$+ P \left[f(\overline{x}, \overline{u}, \overline{\nu}) + \Gamma \delta \nu + B(\tilde{u} - \overline{u}) \right] -$$

$$- Q(\tilde{x} - \overline{x}) \quad b(T) = 0,$$

$$u_{\text{subopt}} = -R^{-1}B^T P \delta x - R^{-1}B^T b + \tilde{u}. \qquad (22)$$

References

H. Chen and F. Allgöwer. A quasi-infinite horizon nonlinear model predictive control scheme with guaranteed stability. *Automatica*, 34(10):1205–1217, 1998.

L. Davis. *Handbook of Genetic Algorithms*. Van Nostrand Reinhold, 1991.

G. Fiengo, L. Glielmo, and S. Santini. On board diagnosis for three-way catalytic converters. *International Journal of Robust Nonlinear Control*, 11:1073–1094, 2001.

G. Fiengo, L. Glielmo, S. Santini, and G. Serra. Control oriented models for twc-equipped spark ignition engines during the warm-up phase. *accepted to 2002 American Control Conference*, 2002.

D. Q. Mayne and H. Michalska. Receding horizon control of nonlinear systems. *IEEE Transaction on Automatic Control*, 35(7):814–824, 1990.